Published in final edited form as:

Nature. 2015 July 30; 523(7562): 597–601. doi:10.1038/nature14553.

Parent stem cells can serve as niches for their own daughter cells

Ana Pardo-Saganta[#1,2,3], **Purushothama Rao Tata**[#1,2,3], **Brandon M. Law**[1,2,3], **Borja Saez**[1,3,4], **Ryan Dz-Wei Chow**[1,2,3], **Mythili Prabhu**[1,2,3], **Thomas Gridley**[5], and **Jayaraj Rajagopal**[1,2,3,**]

[1] Center for Regenerative Medicine, Massachusetts General Hospital, 185 Cambridge Street, Boston, Massachusetts 02114, USA

[2] Departments of Internal Medicine and Pediatrics, Pulmonary and Critical Care Unit, Massachusetts General Hospital, Boston, Massachusetts 02114, USA

[3] Harvard Stem Cell Institute, Cambridge, Massachusetts 02138, USA

[4] Stem Cell and Regenerative Biology Department, Harvard University, Cambridge, Massachusetts 02138, USA

[5] Center for Molecular Medicine, Maine Medical Center Research Institute, 81 Research Drive, Scarborough, Maine 04074, USA.

[#] These authors contributed equally to this work.

Stem cells integrate inputs from multiple sources. Stem cell niches provide signals that promote stem cell maintenance[1-2], while differentiated daughter cells are known to provide feedback signals to regulate stem cell replication and differentiation[3-6]. Recently, stem cells have been shown to regulate themselves using an autocrine mechanism[7]. The existence of a "stem cell niche" was first postulated by Schofield in 1978[1]. Since then, an ever increasing body of literature has focused on defining stem cell niches[1-6]. Yet, little is known about how progenitor cell and differentiated cell numbers and proportions are maintained. In the airway epithelium, basal cells function as stem/progenitor cells that can both self-renew and produce differentiated secretory cells and ciliated cells[8,9]. Secretory cells also act as transit-amplifying cells that eventually differentiate into post-mitotic ciliated cells[9,10] (Extended Data Fig. 1a). Here we describe a mode of cell regulation in which adult mammalian stem/progenitor cells relay a forward signal to their own progeny. Surprisingly, this forward signal is shown to be necessary for daughter cell maintenance. Using a combination of cell ablation, lineage tracing, and signaling pathway modulation, we show that airway basal

[**]**Correspondence:** Jayaraj Rajagopal, MD, Center for Regenerative Medicine, Massachusetts General Hospital, Simches, 4.240, 185 Cambridge Street, Boston, MA 02114, USA. Phone: 617-803-9740; Fax: 617-724-2662; jrajagopal@mgh.harvard.edu..

Author contribution: A.P-S. designed and performed the experiments and co-wrote the manuscript; P.R.T performed the ablation experiments and edited the manuscript; B.M.L. optimized the immunodetection of N2ICD, analyzed the phenotype of *RBPJk* and *Mib1* deletion *in vivo*, and co-wrote the manuscript; B.S. performed flow cytometry experiments and analysis, contributed to the *in vitro* experiments and edited the manuscript; R.C. and M.P. helped with the analysis of the *in vivo* experiments; J.R. suggested and co-designed the study and co-wrote the manuscript.

stem/progenitor cells continuously supply a Notch ligand to their daughter secretory cells. Without these forward signals, the secretory progenitor cell pool fails to be maintained and secretory cells execute a terminal differentiation program and convert into ciliated cells (Extended Data Fig. 1b). Thus, a parent stem/progenitor cell can serve as a functional daughter cell niche (Extended Data Fig. 1c, d).

To establish whether post-mitotic ciliated cells send a conventional feedback signal to regulate the replication of their parent stem and progenitor cells, we genetically ablated ciliated cells using *FOXJ1-creER; LSL-DTA* mice (herein referred to as FOXJ1-DTA) (Fig. 1a). Following ciliated cell ablation, the absolute numbers and morphology of secretory progenitor cells (SCGB1A1$^+$) and basal stem/progenitor cells (CK5$^+$) remained unchanged despite the ablation of 78.8% of ciliated cells (On day-5, 24.29 ± 0.3% of all DAPI$^+$ epithelial cells in control mice were FOXJ1$^+$ ciliated cells *vs* 5.13 ± 0.4% in tamoxifen-treated mice (n=3 mice)) (Fig. 1bc and Extended Data Fig 2a, b). Surprisingly, we did not observe the anticipated increase in stem or progenitor cell proliferation and/or their differentiation to replenish missing ciliated cells (Extended Data Fig. 2c-e). Even over extended periods of time, the rates of epithelial proliferation remained similar to those of uninjured controls (Extended Data Fig. 2d). Indeed, the number of ciliated cells increased at a rate that corresponds to the normal rate of ciliated cell turnover (Fig. 1d). Following ciliated cell ablation, ciliated cell turnover occurs with a half-life of 149 days (Fig. 1e) which mirrors the reported steady-state half-life of approximately 6 months[11]. Additionally, the mesenchymal, hematopoietic, endothelial, and smooth muscle cell populations appeared unchanged (Extended Data Fig. 2f,g).

Lacking evidence to support the presence of a feedback mechanism to restore ciliated cell numbers after ablation, we wondered whether basal stem/progenitor cells might regulate secretory daughter cell behavior by regulating the differentiation of secretory cells into ciliated cells. Thus, we ablated basal cells and simultaneously traced the lineage of secretory progenitor cells using *Scgb1a1-creER;LSL-YFP;CK5-rtTA;tet(O)DTA* mice (hereafter referred to as SCGB1A1-YFP;CK5-DTA) as previously described[12] (Fig. 1f). In addition to the dedifferentiation of secretory cells we previously described following stem cell ablation[12], we observed an increase in lineage labeled YFP$^+$ cells expressing the ciliated cell marker FOXJ1 (8.1 ± 1.6% of YFP$^+$ cells were FOXJ1$^+$ in controls *vs.* 42.4 ± 1.0% in experimental animals) and an accompanying decrease in YFP$^+$ SCGB1A1$^+$ secretory cells (88.5 ± 4% *vs.* 45 ± 3%) (n=3 mice) (Fig. 1g, h). Additionally, we again observed that ~8% of lineage labeled secretory cells dedifferentiated into basal cells as previously described[12]. Thus, we can now account for the fates of all lineage labeled secretory cells after stem cell ablation since the decrement in secretory cell lineage label (43.5%) is almost precisely equal to the combined increase in lineage labeled ciliated and basal cells (34% and 8% respectively). Importantly, lineage labeled ciliated cells expressed C-MYB, a transcription factor required for ciliogenesis[13,14] and acetylated-tubulin (ACTUB) confirming that secretory cells differentiated into mature ciliated cells (Extended Data Fig. 3a, b). These results were further confirmed by flow cytometry (Extended Data Fig. 3c). In contrast to the aforementioned changes in the tracheal epithelium in which the total number of ciliated cells increased 2-fold (625 ± 29 *vs.* 1208 ± 93 ciliated cells, representing 24.5 ± 1.5% and 61 ±

4.7% of total cells respectively) (Extended Data Fig. 3d), the underlying mesenchyme remained unchanged in morphology and its complement of hematopoietic, endothelial, and smooth muscle cells (Extended Data Fig. 3e, f).

Since the Notch pathway has been shown to regulate ciliated *versus* secretory cell fate choices in the embryonic lung and regenerating adult airway epithelium[15–20], we next assessed the expression of Notch pathway components in each cell type of the adult homeostatic airway epithelium. Quantitative RT-PCR analysis on purified airway epithelial cells revealed that the Notch1 receptor was highly expressed in basal stem/progenitor cells as previously reported[18], Notch2 and Notch3 were significantly enriched in secretory progenitor cells, and Notch4 was not detected (n=3 mice) (Fig. 2a and Extended Data Fig. 4a).

Signaling through the Notch2 receptor has previously been postulated to regulate secretory cell fate in the embryonic lung[19], in inflammatory cytokine-induced goblet cell metaplasia[20], and we have found it to be activated during secretory cell fate commitment during regeneration[21]. Interestingly, we found that steady-state nuclear Notch2 intracellular domain (N2ICD) expression was restricted to secretory progenitor cells (92.7 ± 8% of $N2ICD^+$ cells were secretory cells. n=3 mice) while negligible amounts of N2ICD were detected in basal stem/progenitor cells (1.5 ± 3%) and none was seen in ciliated cells (Fig. 2a-e). Consistently, 85.1 ± 5.9% of $SSEA\text{-}1^+$ cells and 93.7 ± 2.1% of $SCGB1A1^+$ cells demonstrated active N2ICD expression (Fig. 2b-e). To further confirm these observations, we stained airway sections from B1–eGFP mice (in which eGFP is expressed exclusively in secretory cells)[12,22], and found that 92.6 ± 2.2% of $eGFP^+$ cells co-expressed N2ICD (Fig. 2f, g). Contrary to the cell specificity associated with N2ICD, we found activated Notch1 (N1ICD) was expressed in most basal stem/progenitor cells and secretory progenitors (Extended Data Fig. 4b). Active N3ICD was detected in subsets of basal, secretory and ciliated cells (Extended Data Fig. 4c). Additionally, the Notch target genes *Hey1* and *HeyL* were enriched in secretory progenitor cells (Extended Data Fig. 4d).

To directly test whether sustained tonic Notch activation is required to maintain secretory cell fate, we abrogated Notch signaling in these cells using *Scgb1a1-creER; LSL-YFP; RBPJk*$^{fl/fl}$ mice (hereafter referred to as SCGB1A1-RBPJk$^{fl/fl}$). The efficient deletion of *RBPJk*, an essential transcription factor required for canonical Notch signaling[23], was confirmed (Extended Data Fig. 5a-c). As a consequence of *RBPJk* deletion, the Notch target genes *Hes1* and *HeyL* were downregulated (Extended Data Fig. 5c). Of note, there is a population (approximately 20%) of YFP^+ secretory cells in which *RBPJk* deletion has not occurred (yellow arrows in Extended Data Fig. 5a), accounting for the residual *RBPJk* message (Extended Data Fig. 5c). We next assessed the fate of lineage labeled secretory cells following RBPJk loss (Fig. 3a) and found that YFP^+ cells were less likely to express secretory cell markers SCGB1A1 (94.4 ± 0.9% *vs.* 31.3 ± 2.2% of YFP^+ cells), SCGB3A2 (93.6 ± 1.2% *vs.* 25.7 ± 2.3%) and SSEA-1 (90 ± 1.7% *vs.* 23.5 ± 1%) at the protein level, and were more likely to express the ciliated cell proteins FOXJ1 (5.1 ± 0.6% *vs.* 68.2 ± 3.1%), ACTUB (7.4 ± 1.3% *vs.* 70.6 ± 3.8%) and C-MYB (n=6 mice) (Fig 3b,c and Extended Data Fig. 5d,e). A decrease in the expression of the secretory cell-specific genes *Scgb1a1* and *Scgb3a2* and an increase in the expression of the ciliated cell genes *FoxJ1* and

c-Myb in lineage labeled YFP$^+$ cells was also observed (n=3 mice) (Fig. 3d). Similarly, secretory cells that had undergone recombination and lost RBPJk concomitantly lost their characteristic N2ICD expression as they switched fate into FOXJ1$^+$ ciliated cells (Fig. 3e). Less than 0.1% of YFP$^+$ cells co-expressed CK5, suggesting that the lack of Notch signaling in secretory cells is not responsible for the dedifferentiation of secretory cells into basal cells that we previously described following basal cell ablation[12] (Extended Data Fig. 5f, g). The cell fate changes described above were confirmed by flow cytometry (Extended Data Fig. 5h, i) and the phenotype persisted over time (Extended Data Fig. 6a-e). Moreover, overall airway cell proliferation and apoptosis were not affected by RBPJk loss (Extended Data Fig. 6f-k). RBPJk loss induced the direct differentiation of secretory cells into ciliated cells in the absence of proliferation since only 1.7 ± 1.1% of all FOXJ1$^+$ cells had incorporated BrdU over the course of the experiment (Extended Data Fig. 6f) and not a single BrdU$^+$ YFP$^+$ FOXJ1$^+$ ciliated cell was found following continuous BrdU administration (Extended Data Fig. 6h, i). In aggregate, these results suggest that tonic canonical Notch activity in secretory progenitor cells is necessary for their continued maintenance at steady-state, and that Notch acts by preventing the differentiation of the secretory progenitor cell pool into the terminally differentiated post-mitotic ciliated cell pool.

To determine whether secretory cell-specific N2ICD transduces a putative basal cell signal that is required for the maintenance of the secretory cell pool, we deleted *Notch2* from secretory cells using *Scgb1a1-creER;LSL-YFP;Notch2$^{fl/fl}$* mice (hereafter referred to as SCGB1A1-Notch2$^{fl/fl}$) (Fig. 3a). We first confirmed the efficient deletion of *Notch2* and the downregulation of *Hes1* and *HeyL (*Extended Data Fig. 7a-d). Upon *Notch2* deletion, we observed that lineage labeled cells ceased to express the secretory cell markers SCGB1A1 (95.6 ± 1.5% *vs*. 23.8 ± 3%), SCGB3A2 (90.8 ± 1.3% *vs.* 6.8 ± 1%) and SSEA-1 (88.2 ± 2.8% *vs.* 22.7 ± 1%) and acquired the expression of the ciliated cell markers FOXJ1 (5.7 ± 2.1% *vs.* 78 ± 0.7%), acetylated-tubulin (3.7 ± 1.9% *vs.* 57.6 ± 6%) and C-MYB (5.6 ± 0.4% *vs.* 84.5 ± 2.3%) (n=7 mice) (Fig. 3f,g and Extended Data Fig. 7e,f). Consistently, the expression of secretory cell genes (*Scgb1a1* and *Scgb3a2*) was downregulated in lineage labeled cells while ciliated cell genes (*FoxJ1* and *c-myb*) were upregulated (n=3 mice) (Fig. 3h). Intriguingly, YFP staining was present in the actual cilia of lineage labeled cells, consistent with the terminal differentiation of secretory cells into mature ciliated cells (Fig. 3f,i). Flow cytometry analysis confirmed these cell fate transitions (Extended Data Fig. 7g, h) and also confirmed a lack of dedifferentiation of secretory cells into basal stem cells following Notch pathway modulation (Extended Data Fig. 7i, j). The observation that N2ICD and FOXJ1 expression remained mutually exclusive following *Notch2* deletion also suggested a largely completed cell fate transition (Fig. 3i). However, very rarely, YFP$^+$ cells expressing both markers were observed, leading one to speculate that these rare cells are evanescent transitioning cells caught in the process of differentiating from a secretory cell into a ciliated cell (Extended Data Fig. 8a). Similarly, rare lineage labeled cells also co-express SSEA-1 and FOXJ1 (Extended Data Fig. 8b). Furthermore, following Notch2 elimination, Ki67 and BrdU incorporation and rates of apoptosis remained unchanged (Extended Data Fig. 8c-g). Additionally, secretory cells directly differentiated into ciliated cells in the absence of proliferation since an insignificant 1.4 ± 1.7% of FOXJ1$^+$ cells were BrdU$^+$ following continuous BrdU administration (Extended Data Fig. 8d, e). Altogether,

these data demonstrate that tonic Notch2 activity within secretory cells is required for the maintenance of secretory cells. Based upon the results of the basal cell ablation, we speculated that the Notch signal-sending cells are basal stem/progenitor cells.

Consistent with prior studies[8,16,18,24], we found that *Dll1* and *Jag2* were expressed in basal stem/progenitor cells while *Jag1* was enriched in ciliated cells (Fig. 4a), and *Dll3* and *Dll4* were undetectable (data not shown). To remove the putative Notch signal arising from basal stem/progenitor cells, we deleted *Mindbomb1* (Mib1) which is an E3 ubiquitin ligase required for the normal endocytic processing of all Notch ligands[25] in basal cells using *CK5-rtTA; tet(O)Cre; Mindbomb1f$l^{/fl}$* mice (hereafter referred to as CK5-Mib1$^{fl/fl}$) (Fig. 4b). Upon efficient removal of Mib1 (93.3 ± 3.8% of basal cells) (Extended Data Fig. 9a,b), a decrease in SCGB1A1^{+} (42.8 ± 0.9% *vs.* 26.2 ± 1.0%), SCGB3A2^{+} (44.6 ± 6.6% *vs.* 6.2 ± 0.7%) and SSEA-1^{+} secretory cells (49.2 ± 2.6% *vs.* 24.7 ± 1.1%) was accompanied by an increase in FOXJ1^{+} (30.1 ± 0.9% *vs.* 36.1 ± 1.0%), ACTUB^{+} (21.7 ± 0.7% *vs.* 24.8 ± 0.7%), and C-MYB^{+} ciliated cells (30.8 ± 2.9% *vs.* 56.2 ± 8.0%) (n=4 mice) (Fig. 4c,d and Extended Data Fig. 9c,d). A corresponding significant decrease in the percentage of N2ICD^{+} secretory cells was observed (43 ± 1.7% *vs.* 29.6 ± 0.8% of total epithelial cells) (Fig. 4e, f), confirming that Notch ligands emanating from stem cells are necessary for N2ICD activity in secretory cells. These results were confirmed by flow cytometry which additionally revealed that there were no changes in the abundance of basal cells (Extended Data Fig. 9e, f). Rates of proliferation and apoptosis were also unchanged (Extended Data Fig. 9g-l) and a negligible 0.77 ± 1.5% of FOXJ1^{+} cells were found to incorporate BrdU after continuous BrdU administration (Extended Data Fig. 9i, j). In addition, the cell fate changes described above continued to be present 5 weeks after *Mib1* deletion (Extended Data Fig. 9m).

All of these results point to the notion that basal stem/progenitor cells send an essential signal to secretory progenitor cells, and that this signal is necessary for the maintanence of the appropriate balance of cell types in the airway epithelium. Since Jag2 is the most abundantly expressed ligand in basal stem cells (Fig. 4a), we knocked down *Jag2* expression *in vitro* using shRNA lentiviral vectors (Extended Data Fig. 10a-c). This resulted in a decrease in *Scgb1a1* and *Scgb3a2* expression and an increase in *FoxJ1* and *c-myb* expression (Extended Data Fig. 10d), resembling the effects of *in vivo* Notch signaling disruption. To confirm that Jag2 is indeed the signal emanating from basal stem/progenitor cells, we generated *CK5-creER; LSL-YFP; Jagged2$^{fl/fl}$* mice (hereafter referred to as CK5-Jag2$^{fl/fl}$) to genetically remove Jag2 from basal stem/progenitor cells *in vivo* (Fig. 4a). *Jag2* deletion was confirmed (Extended Data Fig. 10e) and although the efficiency of recombination as judged by the number of YFP^{+} recombined cells was approximately 10% (Extended Data Fig. 10f), the deletion caused a dramatic decrease in N2ICD^{+} suprabasal cells (43 ± 6.6% *vs.* 17 ± 4.5% of total airway epithelial cells) (Fig. 4g,h) confirming that Jag2 is the basal cell signal responsible for activating N2ICD in secretory cells. Consistently, we observed a decrease in SCGB1A1^{+} (63 ± 2.1% *vs.* 44.4 ± 3.3%), SCGB3A2^{+} (55 ± 7% *vs.* 17.5 ± 0.5%) and SSEA-1^{+} secretory cells (42.8 ± 2% *vs.* 21.8 ± 2%) and a concomitant increase in FOXJ1^{+} (31.3 ± 3.6% *vs.* 46.6 ± 2.2%), ACTUB^{+} (21.7 ± 2.1% *vs.* 46.2 ± 3.9%) and C-MYB^{+} ciliated cells (28.2 ± 2.1% *vs.* 49.6 ± 11.3%) (n=5 mice) (Fig. 4i,j and Extended Data Fig. 10g,h). Results were further confirmed by flow cytometry (Extended Data Fig. 10i, j).

Furthermore, we found no difference in the percentage of $p63^+$ basal cells (Extended Data Fig. 10k, l). Again, N2ICD and FOXJ1 expression was mutually exclusive, consistent with a completed cell fate transition (Extended Data Fig. 10m), and there were no differences in proliferation and apoptosis (Extended Data Fig. 10 n-r).

Taken together, our results show that basal stem/progenitor cells regulate the maintenance of their own progeny through a mechanism in which basal stem cell-produced Jag2 activates Notch2 in daughter secretory progenitor cells to prevent secretory cell differentiation into post-mitotic ciliated cells.

Schofield first introduced the term “niche” to make sense of experimental evidence that suggested the presence of local environments necessary for the maintenance of hematopoietic stem cells[1]. But, he was explicit in referring to “stem cell niches”. We now show that stem/progenitor cells themselves serve as “daughter cell niches”. We would like to suggest that reciprocal forms of niche-type regulation may be a general feature of many tissues in which stem, progenitor, and differentiated cells might all regulate the maintenance of one another.

In order to serve as a progenitor cell niche, airway stem/progenitor cells employ a “forward signal” sent to their own progeny. We define a “forward signal” as a signal that is relayed from a parent cell to its daughter cell. Interestingly, in parallel to our mammalian example, in the fly midgut, a forward Notch signal is sent from an intestinal stem cell to alter the fate choice of its own downstream progeny[26]. However, from one setting to the next, Notch, with its myriad receptors and ligands, will inevitably be deployed in very divergent ways, even within the same tissue[23,24,27,28]. For example, following injury, airway basal stem/progenitor cells use a mechanism akin to lateral inhibition to segregate their lineages[21], whereas pan-epithelial *Jag2* deletion alters the distribution of airway progenitors in the embryonic airway epithelium and here Notch3 is suggested as the relevant receptor[24]. Of note, we identify Notch2 as the receiving receptor on secretory cells. Interestingly, N2ICD is, to the best of our knowledge, the first transcription factor that has been found to be specific to steady-state adult airway secretory progenitor cells.

More generally, we note that differentiated cells are commonly thought to send back signals to their respective stem and progenitor cells to regulate their proliferation and differentiation[3-6]. This process is generally termed feedback regulation, and we were befuddled not to see evidence of such a regulatory mechanism following ciliated cell ablation. More recently, self signals have been identified that mediate autocrine stem cell regulation[7]. Since we demonstrate the existence of a “forward signal,” we would like to suggest that “forward regulation” by stem cells is likely to exist (Extended Data Fig. 1d). While it is tempting to call this form of regulation “feed-forward regulation” to contrast it to “feedback regulation”, this term has been used in control theory to denote a more complex form of regulation that involves 3 discrete entities that interact in a loop[29,30]. Therefore, we opt to coin the simpler term “forward regulation”. To illustrate what we intend to suggest, we note that Notch signals in fly intestinal stem cells occur at varying levels that in turn determine daughter cell fate[26]. Thus, it stands to reason that the regulation of these forward Notch signals could be employed to alter the distribution of daughter cell types. In our case,

perhaps fluctuations in basal cell ligand levels determine the rate of ciliated cell turnover? And how would such forward signals be modulated following tissue injury? A recent study points to Notch2 as a receptor relevant to human asthma[20]. Perhaps increasing basal cell ligand concentration is a mechanism used to engender the asthmatic epithelial phenotype in which secretory daughter cells differentiate into mucous-secreting goblet cells. Thus, we speculate that stem cells, using forward regulatory mechanisms, may orchestrate many tissue wide changes, rather than merely acting as a source of new cells.

Methods

Animals

FOXJ1-creER[11], *CK5-rtTA*[31], *Scgb1a1-creER*[10], *tet(O)cre* (JAX 006224), *CK5-creER*[32], *tet(O)DTA*[33], *Rosa26R-DTA* (JAX 009669), *RBPJk*$^{fl/fl}$ [34], *LSL-YFP* (JAX 006148), *Mindbomb1*$^{fl/fl}$ [25], *Notch2*$^{fl/fl}$ (JAX 010525), *Jag2*$^{fl/fl}$ [35] and C57BL6/J (JAX 000664) mice were previously described. Progeny of *Scgb1a1-creER* and *LSL-YFP* crosses as well as *CK5-rtTA* and *tet(O)DTA* crosses were subsequently mated to generate *Scgb1a1-creER;LSL-YFP;CK5-rtTA;tet(O)DTA* mice[12]. These mice were treated with tamoxifen and then with inhaled PBS (control) or inhaled Dox as previously described[12]. *Scgb1a1-creER* mice were crossed with *RBPJk*$^{fl/fl}$ mice to generate secretory progenitor specific *Scgb1a1-creER;RBPJk*$^{fl/fl}$ conditional knockout mice. To allow for lineage tracing, these mice were crossed with *LSL-YFP* mice to generate *Scgb1a1-creER;LSL-YFP;RBPJk*$^{fl/fl}$ mice. Tamoxifen was administered by intraperitoneal injection (2 mg per day) for five consecutive days to induce the cre-mediated recombination. Similarly, *Scgb1a1-creER;LSL-YFP;Notch2*$^{fl/fl}$ mice were generated and treated. *CK5-rtTA* and *tet(O)cre* mice were crossed to generate *CK5-rtTA;tet(O)cre* mice. *CK5-rtTA;tet(O)cre* mice were crossed with *Mindbomb1*$^{fl/fl}$ mice to generate basal stem cell specific *CK5-rtTA;tet(O)Cre;Mindbomb1*$^{fl/fl}$ conditional knockout mice. Doxycycline administration was performed through drinking water (1 mg/mL) for 2 weeks as described previously[21,36]. *CK5-creER;LSL-YFP;Jag2*$^{fl/fl}$ mice were generated and treated, in this case with 2 doses of tamoxifen, due to a higher sensitivity of this strain to the compound. Mice were sacrificed 10 days after the last tamoxifen injection. Male 6-12 week old mice were used for experiments except in specific circumstances in which breeding limitations led to the use of females in the following strains: *SCGB1A1-creER;LSL-YFP;CK5-rtTA;tet(O)DTA* and *CK5-rtTA;tet(O)Cre;Mindbomb1*$^{fl/fl}$ mice. Similar aged mice were used for both control and treated animals. Controls include corn oil-treated *FOXJ1-creER*; *tet(O)DTA* mice, i-PBS treated Tam-induced *Scgb1a1-creER;LSL-YFP;CK5-rtTA;tet(O)DTA* mice, Tam-treated *Scgb1a1-creER;LSL-YFP;RBPJk*$^{fl/+}$ mice, Tam-treated *Scgb1a1-creER;LSL-YFP;RBPJk*$^{+l/+}$ mice, Tam-treated *Scgb1a1-creER;LSL-YFP;Notch2*$^{+/+}$ mice, Dox-treated *CK5-rtTA;tet(O)Cre;Mib1*$^{+/+}$ mice and Tam-treated *CK5-creER;LSL-YFP;Jag2*$^{+/+}$ mice. BrdU (5mg) was administered intraperitoneally 2h before sacrifice in all cases. Additionally, we treated mice with 1mg/ml of BrdU in drinking water from the time of the last tamoxifen injection to sacrifice to analyze proliferative events occurring as a consequence of genetic modulation. We analyzed at least 3-7 mice per condition in each experiment and all the experiments were repeated at least three times with the exception of *CK5-rtTA;tet(O)Cre;Mindbomb1*$^{fl/fl}$ and the cell ablationexperiments that were repeated twice.

All procedures and protocols were approved by the MGH Subcommittee on Research Animal Care in accordance with NIH guidelines.

Tissue preparation, immunohistochemistry, and immunofluorescence

Mouse trachea were removed using sterile technique and then fixed in 4% paraformaldehyde for 2 hours at 4°C, washed with PBS, and transferred to a 30% sucrose solution overnight. For immunofluorescence, airways were embedded in OCT and cryosectioned as transverse 7 μm sections. Cryosections were stained with the previously described protocol[12,21,36,37]. The following antibodies were used: rabbit anti-caspase3, cleaved (1:100, 9661, Cell Signaling); rabbit anti-cytokeratin 5 (1:1000; ab53121, Abcam); mouse anti-FOXJ1 (1:500; 14-9965, eBioscience); chicken anti-green fluorescent protein (1:500; GFP-1020, Aves Labs); goat anti-GFP (1:100; NB-100-1770, Novus Biologicals); anti-Ki67 (1:200; ab15580, Abcam); rat anti-RBPJk (1:100; SIM-2ZRBP2, Cosmobio); goat anti-SCGB1A1 (1:500; kindly provided by Barry Stripp); goat anti-CC10 (1:100; sc-9772, Santa Cruz Biotechnology), rabbit anti-SCGB3A2 (1:100; kindly provided by Shioko Kimura); mouse anti-p63 (1:100; sc-56188, Santa Cruz Biotechnology); mouse IgM anti-SSEA-1 (1:100; 14-8813-82, eBioscience), mouse anti-tubulin, acetylated (1:100; T6793, Sigma), rabbit anti-alpha smooth muscle Actin (1:100; ab5694, Abcam), rat anti-CD45 (1:100; 14-0451, eBioscience) and rat anti-CD31 (1:100; 553370, BD Pharmingen). BrdU incorporation was detected using Amersham Cell Proliferation Kit (RPN20, GE Healthcare, Waukesha, WI). Cell death was detected using DeadEnd Fluorometric TUNEL System (G3250, Promega, Madison, WI). Appropriate secondary antibodies (Life Technologies' Alexa Fluor series 488, 594, or 647) were diluted 1:500. In the case of rabbit anti-Notch2 (1:2000; D67C8, Cell Signaling), rabbit anti-activated Notch1 (1:1500, ab8925, Abcam), rabbit anti-Notch3 (1:1500, sc-5593, Santa Cruz Biotechnologies), rabbit anti-c-myb (1:3000; sc-519, Santa Cruz Biotechnology) and rabbit anti-Mindbomb1 (1:500, M6073, Sigma), following primary antibody incubation, sections were washed and incubated with anti-Rabbit-HRP conjugate (1:1000; 170-6514, Bio-Rad) for 1 hour at room temperature followed by tyramide signal amplification. Sections were then washed an incubated for 30 minutes at room temperature with streptavidin-594 (1:1000; S-11227, Life Technologies)[21]. For more information on the protocol to detect low levels of c-myb and N2ICD using tyramide signaling amplification, please refer to the Rajagopal Lab website: http://www.massgeneral.org/regenmed/staff/Rajagopallab.

Microscopy and imaging—Tissue was imaged using an Olympus FluoView FV10i confocal microscope (Olympus Corporation). Cells were manually counted based on immunofluorescence staining of markers for each of the respective cell types[21,37]. Briefly, cell counting was performed on the basis of nuclear staining with DAPI (nuclei) and specific cell markers. Cells were counted using 40x magnification fields (each field represented 250 microns of epithelium) covering the whole tracheal epithelium, from cartilage ring 1 to 10, of each mouse. This includes approximately 1300 – 1800 $DAPI^+$ cells per experiment. In *CK5-creER;LSL-YFP;Jag2*$^{fl/fl}$ mice, given the low (approximately 10%) rate of genetic recombination, we showed images in regions where there were patches of YFP^+ basal cells that had undergone recombination, and therefore *Jag2* deletion. Of note, cell counts were performed manually throughout the entire tracheal epithelium, and were not restricted to

areas of basal cell recombination even in these mice. Images were processed and analyzed using ImageJ/Fiji (NIH) and Adobe Photoshop Creative Suite 5 (Adobe).

Cell dissociation, FACS, and flow cytometry analysis—Airway epithelial cells from trachea were dissociated using papain solution as previously described[37]. Briefly, following trachea removal, airway tissue was cut into small fragments and transferred to a 2 ml solution containing 1ml 100 U of pre-activated papain (Worthington biochemical Corporation, cat. # LK003182) and 1 ml of activation buffer as per the manufacturer's protocol. Tissue fragments were incubated on a shaking platform for 90 minutes at 37°C. the cell suspension was passed through a 70μm cell strainer to remove airway husks and pelleted for 5 minutes at 400g. The supernatant was aspirated and the pellet was resuspended in ovomucoid solution (Worthington biochemical Corporation, cat. # LK003182) for 20 minutes at 4°C to inactivate residual papain activity. Dissociated cells were stained with the following antibodies: EpCAM-PECy7 (1:50; 25-5791-80, eBiosciences) or EpCAM-APC (1:50; 17-5791, eBiosciences); GSIβ4 (Griffonia Simplicifolia Isolectin beta4)-Biotin (L2120, Sigma); SSEA-1 eFluor 650NC (1:75, 95-8813-41, eBiosciences); CD24-PE (1:100, 553262, BD Pharmingen). Primary antibodies were incubated for 30 minutes in 2.5% FBS in PBS on ice. FACS and flow cytometry was performed on a BD FACSAria II sorter at the CRM Flow Cytometry Core (Boston, MA). All aforementioned cell sortings were previously gated for EpCAM to exclusively select epithelial cells. Of note, differences in the percentage of each airway epithelial cell type analyzed by flow cytometry might differ from the quantitation performed by cell counting. This reflects the use of cell surface markers for flow analysis (i.e: CD24 for ciliated cells) in contrast to cell counts based on the nuclear transcription factors (such as FoxJ1 and c-myb for ciliated cells). Additionally, flow cytometry involves enzymatic tracheal dissociation and cells may die in this process and some cell types might demonstrate differential viability following enzymatic dissociation. Sorted cells were lysed immediately in TRI Reagent (Sigma) and RNA was extracted as previously described[37]. Data were analyzed on FlowJo Software (Version 10).

RNA extraction and quantitative RT-PCR—Total RNA was extracted from sorted airway epithelial cells from individual mice to analyze gene expression by quantitative RT-PCR. These procedures were performed as previously described[37]. Relative mRNA expression was normalized to baseline transcript levels in secretory progenitor cells in Figure 2a and 4a, and in control YFP^+ cells in Figure 3d and 3h. In addition, the primer sequences for the following genes were used:

Notch1: Forward 5' tgagactgccaaagtgttgc 3' and reverse 5' gtgggagacagagtgggtgt 3'; *Notch2*: Forward 5' cctgaacgggcagtacattt 3' and reverse 5' gcgtagcccttcagacactc 3'; *Notch3*: Forward 5' tgagtgtccagctggctatg 3' and reverse 5' cacaggtgccattgtgtagg 3'; *Dll1*: Forward 5' ttagcatcattggggctacc 3' and reverse 5' taagtgttggggcgatcttc 3'; *Jag1*: Forward 5' cagtgcctctgtgagaccaa 3' and reverse 5' aggggtcagagagacaagca 3'; *Jag2*: Forward 5' cagatccgagtacgctgtga 3' and reverse 5' ggcttctttgcattctttgc 3'; *Hes1*: Forward 5' ctaccccagccagtgtcaac 3' and reverse 5' atgccgggagctatctttct 3'; *Hey1*: Forward 5' gagaccatcgaggtggaaaa 3' and reverse 5' agcagatccctgcttctcaa 3'; *HeyL*: Forward 5' ccccctttaccctatctcagc 3' and reverse 5' acatggtgggattgggacta 3'; *RBPJk* exon 6-7: Forward 5'

ggcagtggttggaagaaaaa 3' and reverse 5' atgtcatcgctgttgccata 3'; *Notch2* exon3: Forward 5' aacatcgagacccctgtgag 3' and reverse 5' ggctgagcatgtgacaggta 3'; *Jag2* exon2: Forward 5' cgtgtgccttaaggagtacca 3' and reverse 5' gcgaactgaaagggaatgac 3'; *Scgb3a2*: Forward 5'gacaggactgaagaagtgtgtgg 3' and reverse 5' ggaggttgttcacgtagcaaagg 3'; *cmyb*: Forward 5' gctgaagaagctggtggaac 3' and reverse 5' caacgcttcggaccatattt 3'.

Cell culture and Viral Transduction—Mouse tracheal epithelial cells were dissociated with papain and sorted with EpCAM and GSIβ4 as previously described[21,37]. Cells were cultured and expanded in complete SAGM (small airway epithelial cell growth medium; Lonza, CC-3118) using 5mM Rock inhibitor Y-27632 (Selleckbio, S1049). To initiate air–liquid interface (ALI) cultures, airway basal cells were dissociated and seeded onto transwell membranes. After confluence, media was removed from the upper chamber. Mucocilary differentiation was performed with PneumaCult-ALI Medium (StemCell, 05001). Differentiation of airway basal cells on an air–liquid interface was followed by directly visualizing beating cilia in real time after 8 days. One day after plating, mouse basal cells were infected with lentiviral vectors carrying shRNAs targeting mouse *Jag2*. Four different clones were obtained from Sigma (MISSION® shRNA jagged2 NM_010588, clones TRCN0000028858, TRCN0000028871, TRCN0000028877, TRCN0000028906), and cloned into pLKO.1 vector (Addgene Plasmid 10878). Lentiviral production was performed in HEK293 cells following standard protocols. Concentrated viruses were used at a MOI of 6 to infect murine basal cells for 9h at 37C in 5% CO_2, one day after plating. The cells were allowed to grow to confluence before being transferred onto transwell membranes. 23d after ALI initiation, cells were washed, harvested and sorted for GFP and cell specific markers. To assess the efficiency of shRNA Jag2 knockdown, non-purified infected cells were collected 72h after infection and lysed in TRI Reagent.

Statistical analysis—The standard error of the mean was calculated from the average of the indicated number of samples in each case (n=biological replicates/condition/ experiment). All the experiments were repeated at least three times with the exception of *CK5-rtTA;tet(O)Cre;Mindbomb1*$^{fl/fl}$ and the cell ablation experiments that were repeated twice. Data was compared among groups using the Student's t-test (unpaired, two-tailed test). A *p*-value of less than 0.05 was considered significant. The analysis was performed with Prism software (Graphpad Prism version 5.0a).

Extended Data

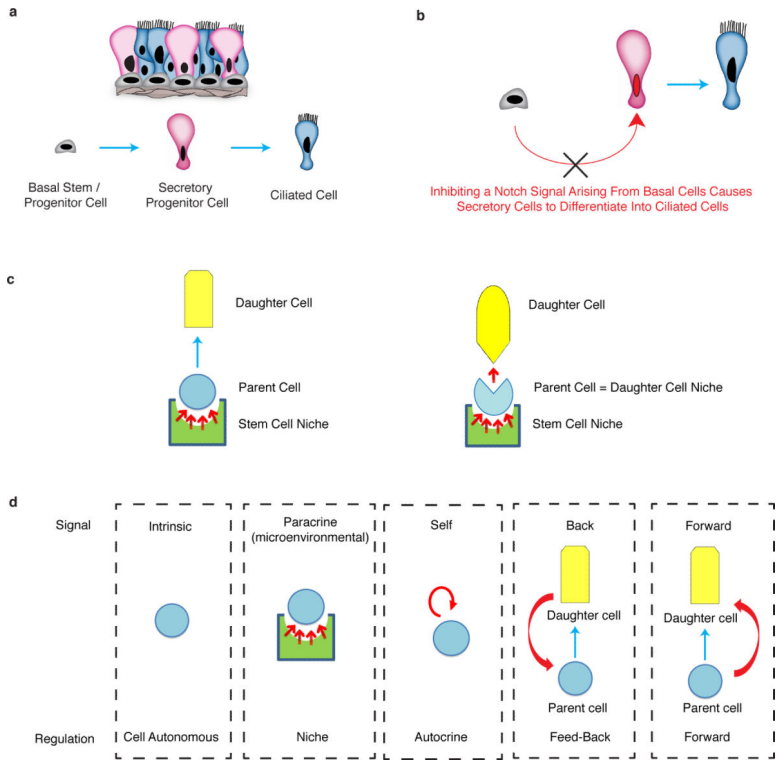

Extended Data Figure 1. Parent stem/progenitor cells can serve as niches for their own daughter cells

a, Schematic representation of the airway epithelial cell lineage. Basal stem/progenitor cells give rise to secretory progenitor cells that, in turn, give rise to terminally differentiated ciliated cells. **b,** Basal cells expressing Notch ligands provide a tonic forward Notch signal to neighboring secretory daughter cells. Blocking this forward signal prevents Notch activation in secretory cells and results in their differentiation into ciliated cells. **c,** On the left, a schematic of the traditional arrangement of a stem cell that is maintained in a stem cell niche. On the right, a schematic that further illustrates that stem cells can themselves serve as daughter cell niches, in which the parent stem cell itself is required for the maintenance of its own progeny. **d,** Schematic of the types of signals that occur between cells within a lineage and the theoretical modes of cell regulation that they imply. Blue arrows indicate a lineage relationship. Red arrows represent signals.

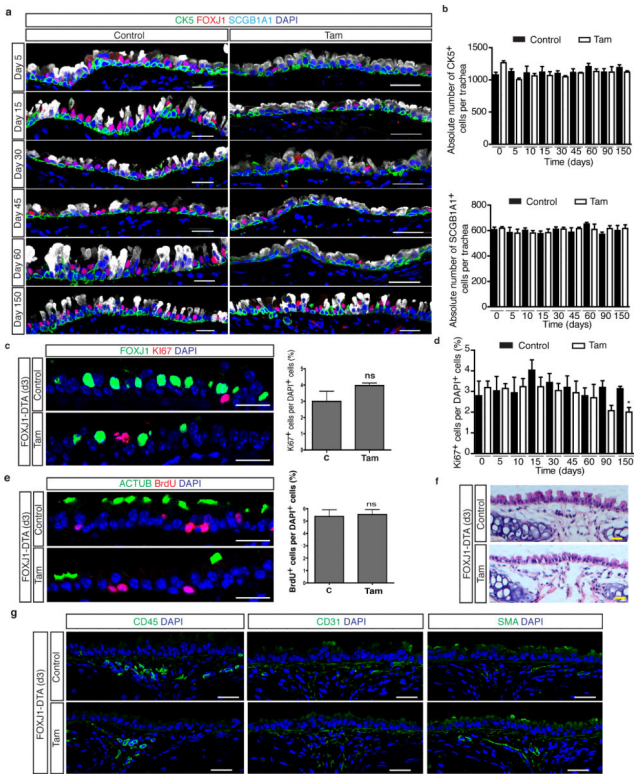

Extended Data Figure 2. Ablation of ciliated cells has no effect on airway cell proliferation, mesenchymal cell types, mesenchymal morphology, and airway stem and progenitor cell replication over time

a, Immunostaining for basal (CK5 (green)), ciliated (FOXJ1 (red)), and secretory cells (SCGB1A1 (white)) on either control (left panels) or tamoxifen (Tam)-treated FOXJ1-DTA mice (right panels) 5, 15, 30, 45, 60, and 150 days after ciliated cell ablation (n=3 mice). **b,** Quantification of absolute cell numbers of basal $CK5^+$ cells (top graph) and secretory $SCGB1A1^+$ cells (bottom graph) per trachea on control (black bars) or Tam-treated (white bars) mice over time (n=3 mice). c, Immunostaining for ciliated cells (FOXJ1 (green)) and proliferating cells (Ki67 (red)) on either control (upper panel) or tamoxifen (Tam)-treated FOXJ1-DTA mice (lower panel) (n=6 mice). On the right, quantification of the percentage of $Ki67^+$ cells per total $DAPI^+$ cells in tracheal sections from control (C) or Tam-treated mice 3 days after cell ablation (n=3 mice). **d,** Quantification of the percentage of proliferating $Ki67^+$ cells relative to total $DAPI^+$ cells in control (black bars) or Tam-treated (white bars) mice over time (n=3 mice). **e,** Immunostaining for ciliated cells (ACTUB (green)) and cells that have undergone proliferation (BrdU (red)) on either control (upper panel) or Tam-treated mice (lower panel) at day 3 (n=6 mice). On the right, quantification of the percentage of $BrdU^+$ cells per total $DAPI^+$ cells in tracheal sections from control (C) or Tam treated mice (n=3 mice). **f,** H&E staining of tracheal sections 3 days after ciliated cell ablation. **g,** Immunostaining for $CD45^+$ hematopoietic cells (left panels), $CD31^+$ endothelial cells (middle panels) and SMA^+ smooth muscle cells (right panels) (green) three days after cell ablation (n=6 mice). Nuclei stained with DAPI (blue). ns indicates that the cell number comparisons are not statistically significant. n=biological replicates/condition. Two independent experiments Data shown in the graphs are means ± SEM. Scale bar, 20μm.

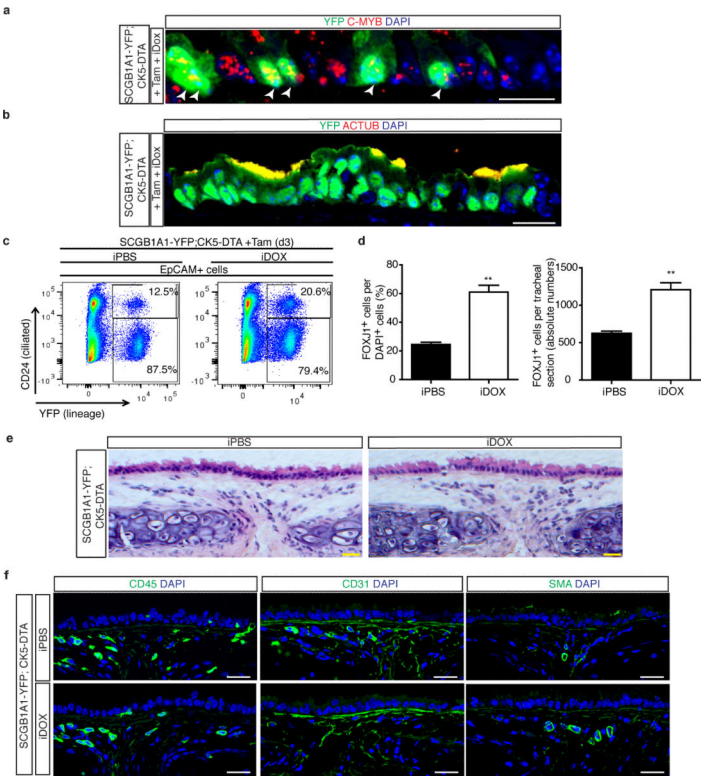

Extended Data Figure 3. Basal stem/progenitor cell ablation promotes the differentiation of secretory cells into ciliated cells without affecting the mesenchyme

a, Immunostaining for YFP lineage label (green) and the ciliated cell marker C-MYB (red) in SCGB1A1-YFP; CK5-DTA mice (n=3 mice). White arrowheads point to double positive cells. **b,** Immunostaining for YFP lineage label (green) and the ciliated cell marker ACTUB (red) using SCGB1A1-YFP; CK5-DTA mice (n=3 mice). **c,** Flow cytometry analysis for lineage labeled YFP^+ cells (x axis) and $CD24^+$ ciliated cells (y axis) cells from control iPBS-treated or Dox-treated SCG1A1-YFP; CK5-DTA mice. **d,** Quantification of the percentage of $FOXJ1^+$ cells per total $DAPI^+$ cells in tracheal sections from control iPBS-treated or iDOX-treated SCG1A1-YFP; CK5-DTA mice (n=3 mice). On the right, absolute numbers of $FOXJ1^+$ cells per tracheal section (n=3 mice). **e,** H&E staining of tracheal sections following basal cell ablation. **f,** Immunostaining for $CD45^+$ hematopoietic cells (left panels), $CD31^+$ endothelial cells (middle panels) and SMA^+ smooth muscle cells (right panels) (green) in control or basal cell-ablated trachea (n=3 mice). All analyses were performed 3 days after cell ablation. Nuclei stained with DAPI (blue). n=biological replicates/condition. Two independent experiments. ** $p<0.01$. Data shown in the graphs are means ± SEM. Scale bar, 20μm.

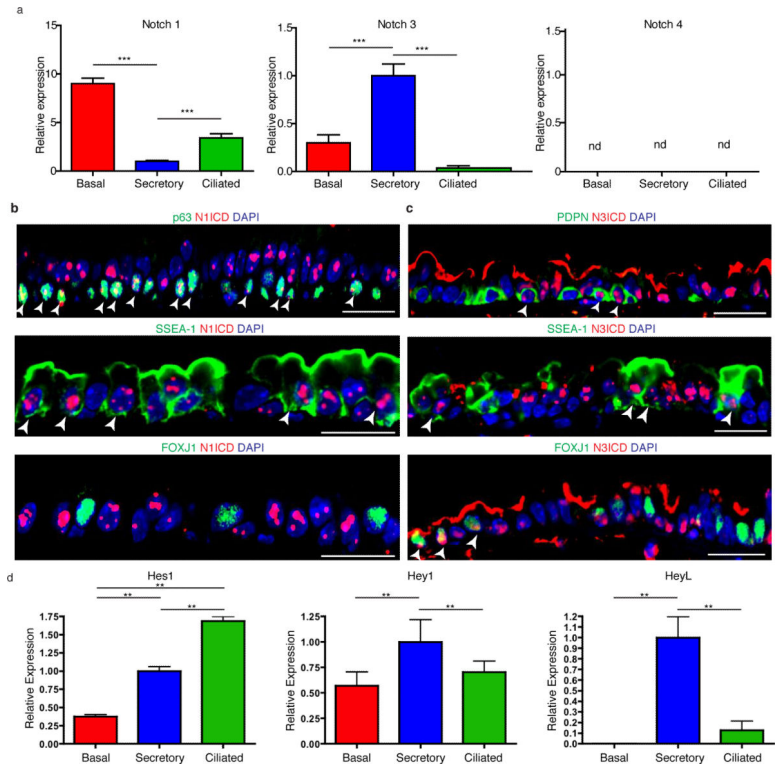

Extended Data Figure 4. Characterization of Notch pathway components in the steady-state murine tracheal epithelium

a, Relative mRNA expression of *Notchl, Notch3* and *Notch4* assessed by qRT-PCR in pure sorted populations of airway epithelial cells (n=3 mice). Relative expression is normalized to baseline transcript levels in secretory progenitor cells. **b,** Immunostaining for N1ICD (red) in combination with the basal cell marker p63 (top panel), the secretory cell marker SSEA-1 (middle panel) and the ciliated cell marker FOXJ1 (bottom panel) (green). **c,** Immunostaining for N3ICD (red) in combination with the basal cell marker podoplanin (PDPN) (top panel), the secretory cell marker SSEA-1 (middle panel) and the ciliated cell marker FOXJ1 (bottom panel) (green). **d,** Relative mRNA expression of *Hes1*, *Hey1* and *HeyL* assessed by qRT-PCR in pure sorted populations of airway epithelial cells (n=3 mice). Relative expression is normalized to baseline transcript levels in secretory progenitor cells. n=biological replicates/condition. ** $p<0.01$; *** $p<0.001$. nd indicates lack of detection. Data shown in the graphs are means ± SEM. Nuclei stained with DAPI (blue). White arrowheads points to double positive cells. Scale bar, 20μm.

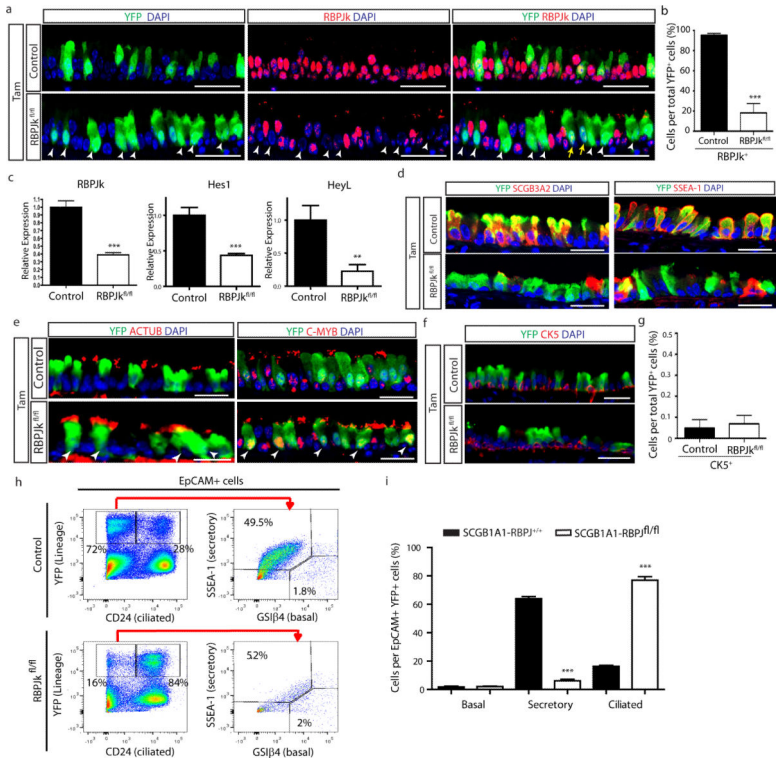

Extended Data Figure 5. Downregulation of Notch signaling transduction following *RBPJk* deletion in secretory progenitor cells induces their conversion into ciliated cells

a, Immunostaining for lineage labeled YFP^{+} cells (green) in combination with RBPJk (red) in Tam-treated SCGB1A1-RBPJk$^{fl/+}$ control mice (upper panels) and Tam-treated SCGB1A1-RBPJk$^{fl/fl}$ mice (lower panels). White arrowheads point to lineage labeled RBPJk^{-} cells. The yellow arrows point to lineage labeled cells that have not undergone recombination. **b,** Quantification of the percentage of RBPJk^{+} cells per total YFP^{+} cells at experimental day 15 following tamoxifen administration to SCGB1A1-RBPJk$^{fl/+}$ control (black bar) and SCGB1A1-RBPJk$^{fl/fl}$ mice (white bar) (n=6 mice). **c,** Relative mRNA expression of Notch signaling component genes (RBPJk, Hes1, HeyL) analyzed by qRT-PCR in sorted YFP^{+} cells from Tam-treated SCGB1A1-RBPJk$^{+/+}$ control mice (black bars) (n=3 mice) and Tam-treated SCGB1A1-RBPJk$^{fl/fl}$ mice (white bars) (n=4 mice). Relative expression is normalized to baseline transcript levels in YFP^{+} control cells. **d,** Immunostaining for YFP lineage label (green) and the secretory progenitor cell markers SCGB3A2 (left panels) and SSEA-1 (right panels) (red) in Tam-treated SCGB1A1-RBPJk$^{fl/+}$ mice (control) (top panels) and SCGB1A1-RBPJk$^{fl/fl}$ mice (bottom panels). **e,** Immunostaining for YFP lineage label (green) and the ciliated cell markers ACTUB (left panels) and C-MYB (right panels) (red) in Tam-treated SCGB1A1-RBPJk$^{fl/+}$ mice (control) (top panels) and SCGB1A1-RBPJk$^{fl/fl}$ mice (bottom panels). White arrowheads point to lineage labeled secretory cells that differentiated into ciliated cells following *RBPJk* deletion. **f,** Immunostaining for lineage labeled YFP^{+} cells (green) and the basal cell marker CK5 (red) on either Tam-treated SCGB1A1-RBPJk$^{fl/+}$ control mice (upper panel) or Tam-treated SCGB1A1-RBPJk$^{fl/fl}$ mice (lower panel). **g,** Quantification of the percentage of CK5^{+} cells per total YFP^{+} cells in Tam-treated SCGB1A1-RBPJk$^{fl/fl}$ mice compared to

control mice. **h,** Flow cytometry analysis of EpCAM^{+} YFP^{+} CD24^{+} lineage labeled ciliated cells and EpCAM^{+} YFP^{+} CD24^{-} SSEA-1^{+} lineage labeled secretory cells or EpCAM^{+} YFP^{+} CD24^{-} GSIC34^{+} lineage labeled basal cells in airways from either control or Tam-treated SCGB1A1-RBPJk$^{fl/fl}$ mice. **i,** Quantification of the percentage of epithelial (EpCAM^{+}) lineage labeled (YFP^{+}) basal, secretory and ciliated cells in either Tam-treated SCGB1A1-RBPJk$^{+/+}$ control or SCGB1A1-RBPJk$^{fl/fl}$ mice by flow cytometry (n=3 mice). The analysis was performed 10 days after the last Tam injection. Images are representative of n=6 mice/condition (biological replicates) repeated three times. Nuclei stained with DAPI (blue). ** p<0.01; *** p<0.001. Data shown in the graphs are means ± SEM. Scale bar, 20μm.

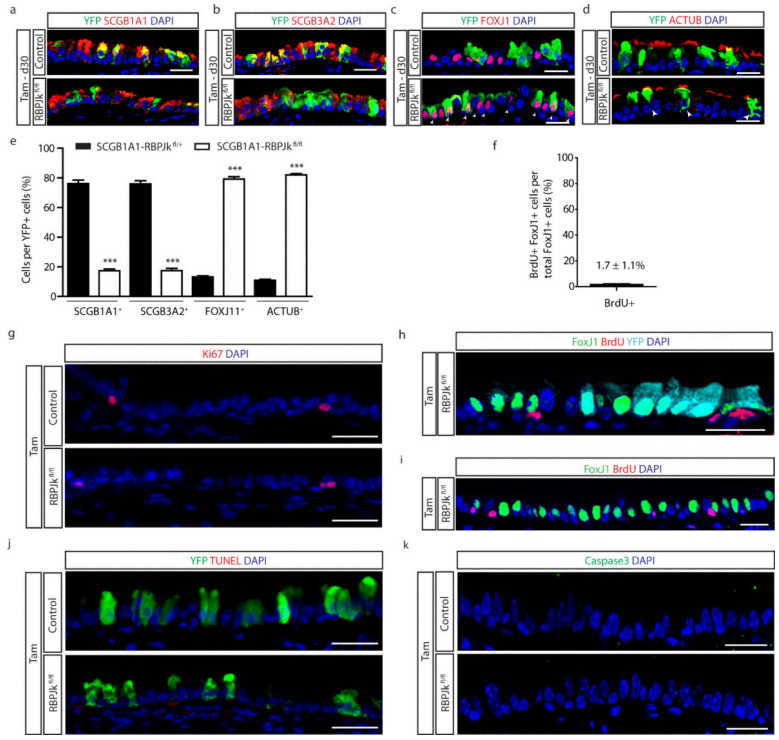

Extended Data Figure 6. Lineage labeled ciliated cells demonstrate long term persistence after *RBPJk* deletion without a change in epithelial cell proliferation and apoptosis

Immunostaining for the lineage label YFP (green) in combination with the secretory cell markers SCGB1A1 **(a),** SCGB3A2 **(b),** or the ciliated cell markers FOXJ1 **(c)** and ACTUB **(d)** (red) on either Tam-treated SCGB1A1-RBPJk$^{fl/+}$ control mice (upper panels) or Tam-treated SCGB1A1-RBPJk$^{fl/fl}$ mice (lower panels) thirty days after the last tamoxifen injection (n=3 mice). White arrowheads point to lineage labeled ciliated cells. **e,** Quantification of the percentage of each cell type per YFP^{+} cells on either control mice (black bars) or Tam-treated SCGB1A1-RBPJk$^{fl/fl}$ mice (white bars) at day 30. **f,** Quantification of the percentage of ciliated FOXJ1^{+} cells that incorporate BrdU after continuous BrdU administration to Tam-treated SCGB1A1-RBPJk$^{fl/fl}$ mice (n=3 mice). **g,** Immunostaining for Ki67 (red) to assess overall proliferation in either Tam-treated SCGB1A1-RBPJk$^{fl/+}$ control mice (upper panel) or Tam-treated SCGB1A1-RBPJk$^{fl/fl}$ mice (lower panel) (n=3 mice). **h,i** Immunostaining for FOXJ1 (green) and BrdU (red) in

combination with YFP (cyan) (h) or alone (i) on Tam-treated SCGB1A1-RBPJk$^{fl/fl}$ mice that received continuous BrdU (n=3 mice). **j,** Immunostaining to detect apoptotic cells by TUNEL assay (red) in combination with YFP lineage labeled cells (green) in either Tam-treated SCGB1A1-RBPJk$^{fl/+}$ control mice (upper panel) or Tam-treated SCGB1A1-RBPJk$^{fl/fl}$ mice (lower panel) (n=3 mice). **k,** Immunostaining for activated caspase3 (green) in control and Tam-treated SCGB1A1-RBPJk$^{fl/fl}$ mice (n=3 mice). **f-k,** Analysis conducted 10 days after induction. Nuclei stained with DAPI (blue). n=biological replicates/condition. *** p<0.001. Data shown in the graph are means ± SEM. Scale bar, 20μm.

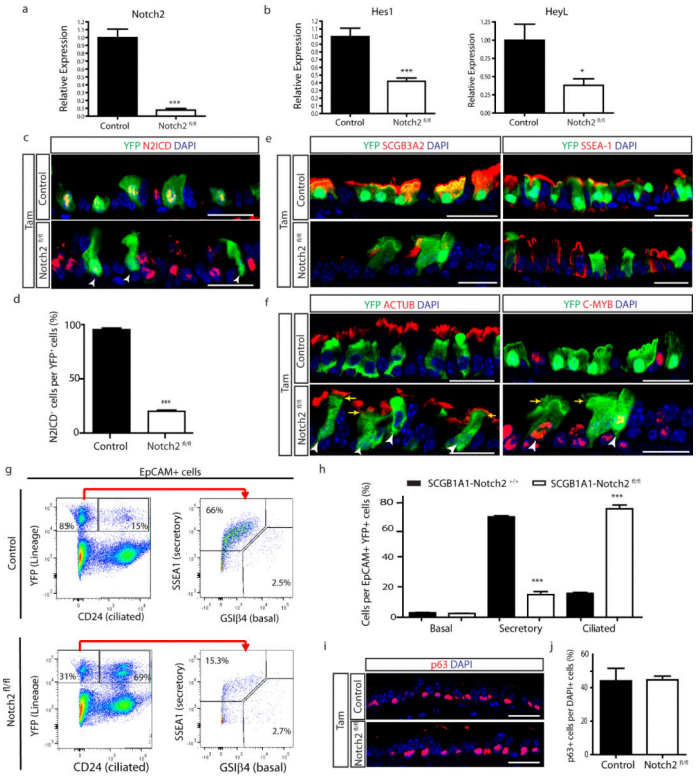

Extended Data Figure 7. Efficient deletion of *Notch2* in secretory progenitor cells and its effect on cell type distribution

a, Relative mRNA expression of *Notch2* in YFP$^+$ cells from Tam-treated SCGB1A1-Notch2$^{+/+}$ control mice and Tam-treated SCGB1A1-Notch2$^{fl/fl}$ experimental mice assessed by qRT-PCR (n=3 mice). **b,** Relative mRNA expression of the Notch target genes (*Hes1*, *HeyL*) in YFP$^+$ cells from control mice and Tam-treated SCGB1A1-Notch2$^{fl/fl}$ experimental mice (n=3 mice). Relative expression is normalized to baseline transcript levels in lineage labeled YFP$^+$ control cells. **c,** Immunostaining for lineage label YFP (green) in combination with N2ICD (red) on control mice (Tam-treated SCGB1A1-Notch2$^{+/+}$) and experimental airways (Tam-treated SCGB1A1-Notch2$^{fl/fl}$). White arrowheads point to lineage labeled cells that had lost Notch2 and therefore do not show N2ICD expression. **d,** Quantification of the percentage of N2ICD$^+$ cells per total YFP$^+$ cells in Tam-treated SCGB1A1-Notch2$^{fl/fl}$ mice compared to control (n=7 mice). **e,** Immunostaining for YFP lineage label (green) and the secretory progenitor cell markers SCGB3A2 (left panels) and SSEA-1 (right panels) (red) in control (top panels) and experimental (bottom panels) mice. **f,** Immunostaining for

YFP lineage label (green) and the ciliated cell markers ACTUB (left panels) and C-MYB (right panels) (red) in control (top panels) and experimental (bottom panels) mice. White arrowheads point to lineage labeled secretory cells that differentiated into ciliated cells following *Notch2* deletion. Yellow arrows point to actual cilia (green) in lineage labeled cells. **g,** Flow cytometry analysis of EpCAM^{+} YFP^{+} CD24^{+} lineage labeled ciliated cells and EpCAM^{+} YFP^{+} CD24^{-} SSEA-1^{+} lineage labeled secretory cells or EpCAM^{+} YFP^{+} CD24-GSIβ4^{+} lineage labeled basal cells in airways from either Tam-treated SCGB1A1-Notch2$^{+/+}$ control mice or Tam-treated SCGB1A1-Notch2$^{fl/fl}$ mice. **h,** Quantification of the percentage of epithelial (EpCAM^{+}) lineage labeled (YFP^{+}) basal, secretory and ciliated cells in either Tam-treated SCGB1A1-Notch2$^{+/+}$ control (n=4 mice) or SCGB1A1-Notch2$^{fl/fl}$ mice (n=6 mice) by flow cytometry. **i,** Immunostaining for the basal cell transcription factor p63 (red) on control or SCGB1A1-Notch2$^{fl/fl}$ airways. **j,** Quantification of the percentage of p63^{+} cells per total DAPI^{+} cells on tracheal sections from control or experimental mice (n=7 mice). Analysis performed 10 days after induction. Images are representative of n=7 mice/condition (biological replicates) repeated three times (three independent experiments). Nuclei stained with DAPI (blue). *p<0.05; *** p<0.001. Data shown in the graphs are means ± SEM. Scale bar, 20μm.

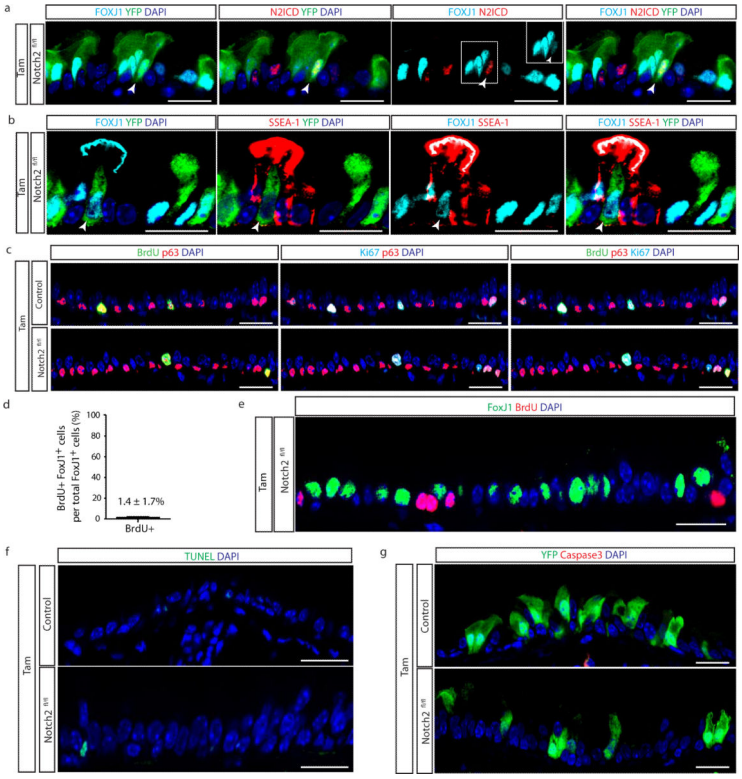

Extended Data Figure 8. Proliferation and apoptosis following deletion of *Notch2* in secretory progenitor cells

a, Immunostaining for lineage label YFP (green), FOXJ1 (cyan) and N2ICD (red) in Tam-treated SCGB1A1-Notch2$^{fl/fl}$ mice. White arrowhead points to a lineage labeled cell co-expressing markers for secretory and ciliated cell fates. The inset shows the single stain for FOXJ1 of the indicated region. **b,** Immunostaining for lineage label YFP (green), FOXJ1

(cyan) and SSEA-1 (red) in Tam-treated SCGB1A1-Notch2$^{fl/fl}$ mice. White arrowhead points to a lineage labeled transitional cell. **c,** Immunostaining for BrdU (green), p63 (red) and Ki67 (cyan) to assess overall proliferation on either Tam-treated SCGB1A1-Notch2$^{+/+}$ control mice (upper panels) or Tam-treated SCGB1A1-Notch2$^{fl/fl}$ mice (lower panels). **d,** Quantification of the percentage of ciliated FOXJ1^{+} cells that incorporate BrdU after continuous BrdU administration to Tam-treated SCGB1A1-Notch2$^{fl/fl}$ mice (n=4 mice). **e,** Immunostaining for FOXJ1 (green) and BrdU (red) on Tam-treated SCGB1A1-Notch2$^{fl/fl}$ mice that received continuous BrdU (n=4 mice). **f,** Immunostaining to detect apoptotic cells by TUNEL assay (green) on either Tam-treated SCGB1A1-Notch2$^{+/+}$ control mice (upper panel) or Tam-treated SCGB1A1-Notch2$^{fl/fl}$ mice (lower panel). **g,** Immunostaining for YFP (green) in combination with activated caspase3 (red) on control mice (upper panel) or Tam-treated SCGB1A1-Notch2$^{fl/fl}$ mice (lower panel). Analysis performed 10 days after induction. Images are representative of n=7 mice/ condition (biological replicates) repeated three times (three independent experiments). Nuclei stained with DAPI (blue). Scale bar, 20μm.

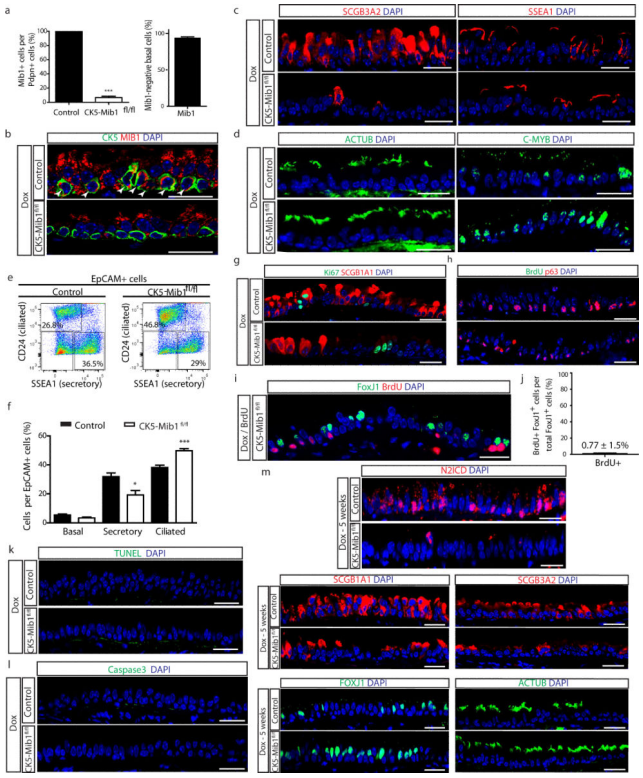

Extended Data Figure 9. Loss of Notch ligands in basal stem cells promotes secretory cell differentiation into ciliated cells without affecting proliferation or apoptosis

a, Quantification of the percentage of basal PDPN^{+} cells that express Mib1 (left graph) on either Dox-treated CK5-Mib1$^{+/+}$ control mice or Dox-treated CK5-Mib1$^{fl/fl}$ mice (n=4 mice). Right graph, percentage of basal cells in which Mib1 was deleted in Dox-treated CK5-Mib1$^{fl/fl}$ mice (n=4 mice). **b,** Immunostaining for Mib1 (red) and the basal cell marker CK5 (green). White arrowheads point to Mib1^{+} basal cells. **c,** Immunostaining for the secretory cell markers SCGB3A2 (left panels) and SSEA-1 (right panels) (red) in control

(top panels) and experimental (bottom panels) mice. **d,** Immunostaining for the ciliated cell markers ACTUB (left panels) and C-MYB (right panels) (green) in control (top panels) and experimental (bottom panels) mice. **e,** Flow cytometry analysis of EpCAM^{+} CD24^{+} ciliated cells and EpCAM^{+} SSEA-1^{+} secretory cells from control and experimental mice. **f,** Percentage of epithelial (EpCAM^{+}) basal, secretory and ciliated cells on both groups by flow cytometry (n=3 mice). **g,** Immunostaining for Ki67 (green) and the secretory cell marker SCGB1A1 (red) on control (top panel) or Dox-treated CK5-Mib1$^{fl/fl}$ mice (bottom panel). **h,** Immunostaining for BrdU (green) in combination with the basal cell transcription factor p63 (red) on both groups. **i,** Immunostaining for FOXJ1 (green) and BrdU (red) on Dox-treated CK5-Mib1$^{fl/fl}$ mice that received continuous BrdU. **j,** Percentage of ciliated FOXJ1^{+} cells that incorporate BrdU after continuous BrdU administration to Dox-treated CK5-Mib1$^{fl/fl}$ mice (n=4 mice). **k,** Immunostaining to detect apoptotic cells by TUNEL assay (green) on either control (upper panel) or experimental mice (lower panel). **l,** Immunostaining for activated caspase3 (green) on both groups). **m,** Immunostaining for N2ICD (red), SCGB1A1 and SCGB3A2 (red), or FOXJ1 and ACTUB (green) in control (top panels) or experimental mice (bottom panels) after five weeks of continuous doxycycline treatment (n=4 mice). **a-l**, Analysis performed 2 weeks after the beginning of Dox induction. Images are representative of n=4 mice/ condition (biological replicates) repeated twice. * p<0.05; *** p<0.001. Data shown in the graphs are means ± SEM. Nuclei, DAPI (blue). Scale bar, 20μm.

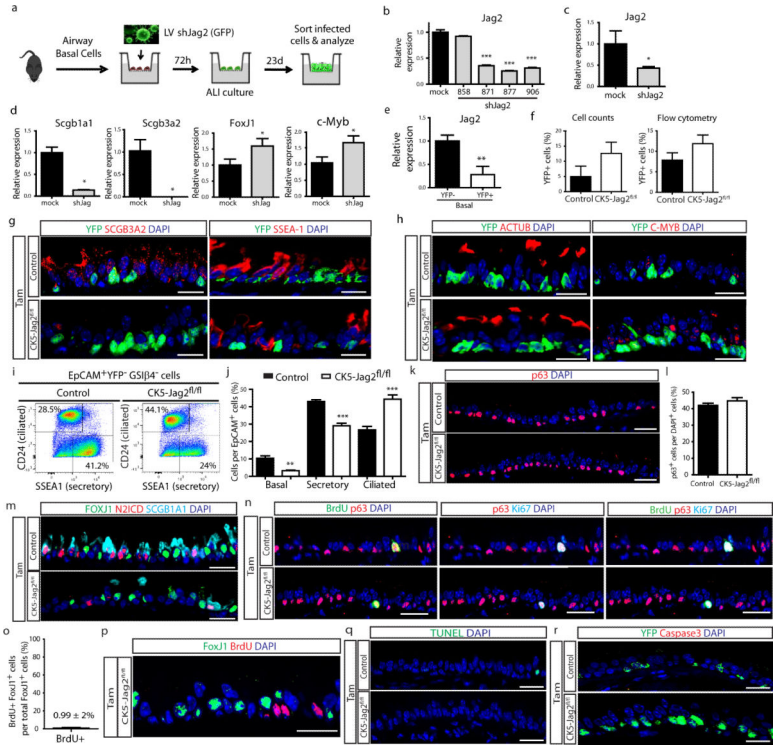

Extended Data Figure 10. Disruption ofDisruption of *Jag2* in basal stem/progenitor cells causes the differentiation of secretory progenitor cells into ciliated cells without affecting proliferation or apoptosis

a, Schematic representation of *Jag2* inhibition using lentiviruses (LV) carrying shRNAs. Infected GFP$^+$ cells were cultured in an air-liquid interface (ALI) culture system for 23d, when they were harvested, sorted and analyzed. **b,** Relative mRNA expression of *Jag2* in tracheal epithelial cells infected with mock vector (control) or with vectors carrying 4 different shRNAs targeting *Jag2* 72h after infection. **c,** Relative mRNA expression of *Jag2* in tracheal epithelial basal cells infected with mock vector (control) or with lentivirus targeting *Jag2* (shJag2 877) after 23d in ALI. **d,** Relative mRNA expression of the secretory genes (*Scgb1a1* and *Scgb3a2*) and the ciliated cell genes (*FoxJ1* and *c-Myb*) in mock (black bars) and shJag2 877 (grey bars) infected cells 23d after ALI initiation. Relative expression is normalized to baseline transcript levels in mock infected cells. **e,** Relative mRNA expression of *Jag2* on sorted recombined (YFP$^+$) basal cells and unrecombined YFP$^-$ basal cells from Tam-treated CK5-Jag2$^{fl/fl}$ mice (n=3 mice). Relative expression is normalized to baseline transcript levels in YFP$^-$ cells. **f,** Percentage of YFP$^+$ cells per total DAPI$^+$ cells (efficiency of recombination) on either Tam-treated CK5-Jag2$^{+/+}$ control (black bars) or Tam-treated CK5-Jag2$^{fl/fl}$ (white bars) mice assessed by manual counting (left graph) (n=5 mice) or by flow cytometry (right graph) (n=3 mice). **g,** Immunostaining for SCGB3A2 (left panels) and SSEA-1 (right panels) (red) in combination with YFP (green) in control (top panels) and experimental (bottom panels) mice. **h,** Immunostaining for ACTUB (left panels) and C-MYB (right panels) (red) in combination with YFP (green) in control (top panels) and experimental (bottom panels) mice. **i,** Flow cytometry analysis of EpCAM$^+$ CD24$^+$ ciliated cells and EpCAM$^+$ SSEA-1$^+$ secretory cells in control and experimental mice. **j,** Percentage of epithelial (EpCAM$^+$) basal, secretory and ciliated cells from both groups assessed by flow cytometry (n=3 mice). **k,** Immunostaining for p63 (red) on control (top panel) and experimental mice (bottom panel). **l,** Percentage of p63$^+$ cells per total DAPI$^+$ cells on both groups. **m,** Immunostaining for FOXJ1 (green), N2ICD (red) and SCGB1A1 (cyan). **n,** Immunostaining for BrdU (green), p63 (red) and Ki67 (cyan) in either control (upper panels) or experimental mice (lower panels). **o,** Percentage of ciliated FOXJ1$^+$ cells that incorporate BrdU after continuous administration of BrdU to Tam-treated CK5-Jag2$^{fl/fl}$ mice (n=3 mice). **p,** Immunostaining for FOXJ1 (green) and BrdU (red) on Tam-treated CK5-Jag2$^{fl/fl}$ mice that received continuous BrdU (n=3 mice). **q,** Immunostaining to detect apoptotic cells by TUNEL assay (green) on both groups. **r,** Immunostaining for YFP (green) in combination with activated caspase3 (red) on control (upper panel) or experimental mice (lower panel). **f-r,** Analysis performed 10 days after induction. Images are representative of n=5 mice/ condition (biological replicates) repeated three times. *p<0.05; **p<0.01; *** p<0.001. Data shown in the graphs are means ± SEM. Nuclei, DAPI (blue). Scale bar, 20μm.

Acknowledgments

We thank Adam Glick for providing the *CK5rtTA* mice, Brigid Hogan for providing *CK5-creER* and *SCGB1A1-creER* mice, and Young-Yun Kong for kindly sharing the *Mib1 floxed* mice. Ben Z Stanger provided the *RBPJk floxed* mice and generously shared protocols for the immunohistochemical detection of Notch components. We also thank Barry Stripp for providing the goat anti-SCGB1A1 antibody. We wish to extend our thanks to all of the members of the Rajagopal Laboratory and the HSCI flow cytometry core facility. This research was supported by the New York Stem Cell Foundation (J.R. is a New York Stem Cell Foundation-Robertson Investigator), by a National Institutes of Health-National Heart, Lung, and Blood Institute Early Career Research New Faculty (P30) award (5P30HL101287-02), an RO1 (RO1HL118185) from NIH-NHLBI (to J.R.) and a Harvard Stem Cell Institute (HSCI) Junior Investigator Grant (to J.R.). J.R. is also the Maroni Research Scholar at MGH.

References

1. Schofield R. The relationship between the spleen colony-forming cell and the haemopoietic stem cell. Blood Cells. 1978; 4:7–25. [PubMed: 747780]
2. Scadden DT. The stem-cell niche as an entity of action. Nature. 2006; 441:1075–1079. [PubMed: 16810242]
3. Hsu YC, Fuchs E. A family business: stem cell progeny join the niche to regulate homeostasis. Nat. Rev. Mol. Cell Biol. 2012; 13:103–114. [PubMed: 22266760]
4. Bruns I, et al. Megakaryocytes regulate hematopoietic stem cell quiescence through CXCL4 secretion. Nat Med. 2014; 20:1315–1320. [PubMed: 25326802]
5. Hsu YC, Li L, Fuchs E. Transit-amplifying cells orchestrate stem cell activity and tissue regeneration. Cell. 2014; 157:935–949. [PubMed: 24813615]
6. Sato T, et al. Paneth cells constitute the niche for Lgr5 stem cells in intestinal crypts. Nature. 2011; 469:415–418. [PubMed: 21113151]
7. Lim X, Tan SH, Koh WL, Chau RM, Yan KS, Kuo CJ, van Amerongen R, Klein AM, Nusse R. Interfollicular epidermal stem cells self-renew via autocrine Wnt signaling. Science. 2013; 342:1226–1230. [PubMed: 24311688]
8. Rock JR, et al. Basal cells as stem cells of the mouse trachea and human airway epithelium. Proc. Natl. Acad. Sci. USA. 2009; 106:12771–5. [PubMed: 19625615]
9. Rock JR, Hogan BLM. Epithelial Progenitor Cells in Lung Development, Maintenance, Repair, and Disease. Annu. Rev. Cell Dev. Biol. 2011; 27:493–512. [PubMed: 21639799]
10. Rawlins EL, et al. The role of Scgb1a1+ Clara cells in the long- term maintenance and repair of lung airway, but not alveolar, epithelium. Cell Stem Cell. 2009; 4:525–534. [PubMed: 19497281]
11. Rawlins EL, Hogan BL. Ciliated epithelial cell lifespan in the mouse trachea and lung. Am J Physiol Lung Cell Mol Physiol. 2008; 295:L231–234. [PubMed: 18487354]
12. Tata PR. Dedifferentiation of committed epithelial cells into stem cells in vivo. Nature. 2013; 503:218–223. [PubMed: 24196716]
13. Pan JH, Adair-Kirk TL, Patel AC, Huang T, Yozamp NS, Xu J, Reddy EP, Byers DE, Pierce RA, Holtzman MJ, Brody SL. Myb permits multilineage airway epithelial cell differentiation. Stem Cells. 2014; 32:3245–3256. [PubMed: 25103188]
14. Tan FE, et al. Myb promotes centriole amplification and later steps of the multiciliogenesis program. Development. 2013; 140:4277–4286. [PubMed: 24048590]
15. Tsao PN, et al. Notch signaling controls the balance of ciliated and secretory cell fates in developing airways. Development. 2009; 136:2297–2307. [PubMed: 19502490]
16. Morimoto M, et al. Canonical Notch signaling in the developing lung is required for determination of arterial smooth muscle cells and selection of Clara versus ciliated cell fate. J. Cell Sci. 2010; 123:213–224. [PubMed: 20048339]
17. Guseh JS, et al. Notch signaling promotes airway mucous metaplasia and inhibits alveolar development. Development. 2009; 136:1751–1759. [PubMed: 19369400]
18. Rock JR, et al. Notch-dependent differentiation of adult airway basal stem cells. Cell Stem Cell. 2011; 8:639–648. [PubMed: 21624809]
19. Morimoto M, Nishinakamura R, Saga Y, Kopan R. Different assemblies of Notch receptors coordinate the distribution of the major bronchial Clara, ciliated and neuroendocrine cells. Development. 2012; 139:4365–4373. [PubMed: 23132245]
20. Danahay H, et al. Notch2 is required for inflammatory cytokine- driven goblet cell metaplasia in the lung. Cell Rep. 2015; 10:239–252. [PubMed: 25558064]
21. Pardo-Saganta A, Law BM, Tata PR, Villoria J, Saez B, Mou H, Zhao R, Rajagopal J. Injury induces direct lineage segregation of functionally distinct airway basal stem/progenitor cell subpopulations. Cell Stem Cell. 2015; 16:184–197. [PubMed: 25658372]
22. Miller RL, et al. V-ATPase B1-subunit promoter drives expression of EGFP in intercalated cells of kidney, clear cells of epididymis and airway cells of lung in transgenic mice. Am. J. Physiol Cell Physiol. 2005; 2204:1134–1144.

23. Kopan R, Ilagan MXG. The canonical Notch signaling pathway: unfolding the activation mechanism. Cell. 2009; 137:216–233. [PubMed: 19379690]
24. Mori M, Mahoney JE, Stupnikov MR, Paez-Cortez JR, Szymaniak AD, Varelas X, Herrick DB, Schwob J, Zhang H, Cardoso WV. Notch3-Jagged signaling controls the pool of undifferentiated airway progenitors. Development. 2015; 142:258–267. [PubMed: 25564622]
25. Koo BK, et al. An obligatory role of Mind Bomb-1 in Notch signaling of mammalian development. PLoS One. 2007; 2:e1221. [PubMed: 18043734]
26. Ohlstein B, Spradling A. Multipotent Drosophila Intestinal Stem Cells Specify Daughter Cell Fates by Differential Notch Signaling. Science. 2007; 315:988–992. [PubMed: 17303754]
27. Stamataki D, Holder M, Hodgetts C, Jeffery R, Nye E, Spencer-Dene B, Winton DJ, Lewis J. Delta1 expression, cell cycle exit, and commitment to a specific secretory fate coincide within a few hours in the mouse intestinal stem cell system. PLoS One. 2011; 6:e24484. [PubMed: 21915337]
28. Ambler CA, Watt FM. Adult epidermal Notch activity induces dermal accumulation of T cells and neural crest derivatives through upregulation of jagged 1. Development. 2010; 137:3569–3579. [PubMed: 20940224]
29. Mangan S, Alon U. Structure and function of the feed-forward loop network motif. Proc Natl Acad Sci U S A. 2003; 100:11980–11985. [PubMed: 14530388]
30. Alon, U. An introduction to systems biology: design principles of biological circuits. Chapman & Hall/CRC; Boca Raton: 2007. ISBN 1- 58488-642-0
31. Diamond I, Owolabi T, Marco M. Conditional gene expression in the epidermis of transgenic mice using the tetracycline-regulated transactivators tTA and rTA linked to the keratin 5 promoter. J. Invest. Dermatol. 2000; 115:788–794. [PubMed: 11069615]
32. Van Keymeulen A, Rocha AS, Ousset M, Beck B, Bouvencourt G, Rock J, Sharma N, Dekoninck S, Blanpain C. Distinct stem cells contribute to mammary gland development and maintenance. Nature. 2011; 479:189–193. [PubMed: 21983963]
33. Weber T, et al. Inducible gene expression in GFAP+ progenitor cells of the SGZ and the dorsal wall of the SVZ-A novel tool to manipulate and trace adult neurogenesis. Glia. 2011; 59:615–626. [PubMed: 21294160]
34. Tanigaki K, et al. Notch-RBP-J signaling is involved in cell fate determination of marginal zone B cells. Nat. Immunol. 2002; 3:443–450. [PubMed: 11967543]
35. Xu J, Krebs LT, Gridley T. Generation of mice with a conditional null allele of the Jagged2 gene. Genesis. 2010; 48:390–393. [PubMed: 20533406]
36. Kim JK, et al. In vivo imaging of tracheal epithelial cells in mice during airway regeneration. Am. J. Respir. Cell Mol. Biol. 2012; 47:864–868. [PubMed: 22984086]
37. Pardo-Saganta A, Law BM, Gonzalez-Celeiro M, Vinarsky V, Rajagopal J. Ciliated cells of pseudostratified airway epithelium do not become mucous cells after ovalbumin challenge. Am. J. Respir. Cell Mol. Biol. 2013; 48:364–373. [PubMed: 23239495]

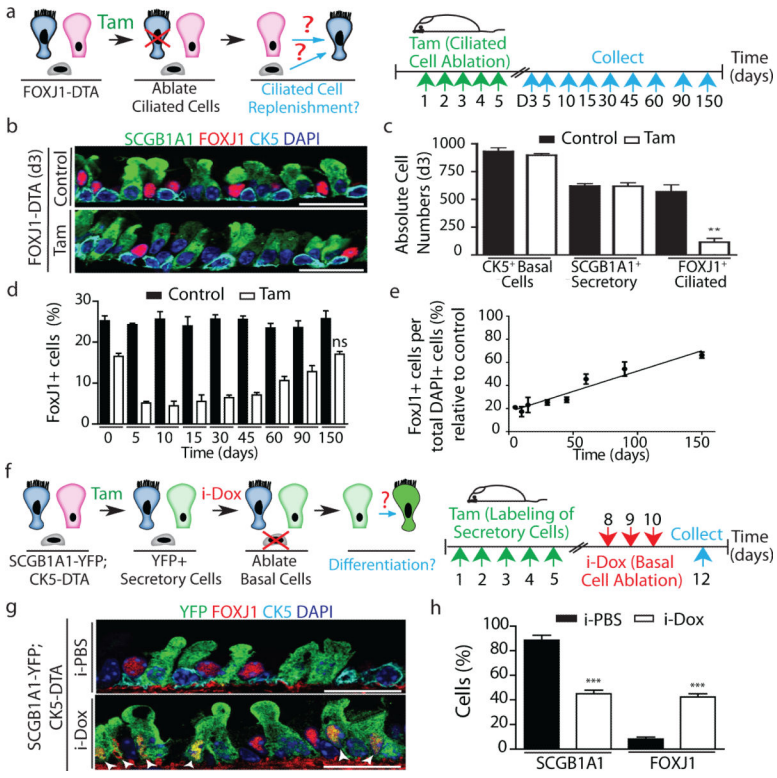

Figure 1. Secretory progenitor cells differentiate into ciliated cells following basal stem/ progenitor cell ablation

a, Schematic representation of ciliated cell ablation. Ciliated, secretory and basal cells are shown in blue, pink and gray respectively. **b,** Immunostaining for SCGB1A1 (green), FOXJ1 (red) and CK5 (cyan) on control (top) or tamoxifen (Tam)-treated FOXJ1-DTA mice (bottom) (n=6 mice). **c,** Absolute cell number of each cell type in both groups (n=3 mice). **d,** Percentage of FOXJ1$^+$ cells per total DAPI$^+$ cells over time (n=3 mice). ns, not significant when compared to day 0 of the same group. **e,** Percentage of FOXJ1$^+$ cells in Tam-treated mice (n=3 mice). **f,** Schematic representation of secretory cell lineage labeling and basal cell ablation. **g,** Immunostaining for FOXJ1 (red), YFP (green) and CK5 (cyan) on i-PBS (top) or i-Dox (bottom) treated SCGB1A1-YFP; CK5-DTA mice (n=3 mice). White arrowheads, lineage labeled ciliated cells. **h,** Percentage of SCGB1A1$^+$ and FOXJ1$^+$ cells per total YFP$^+$ cells. Nuclei, DAPI (blue). n=biological replicates/condition repeated twice (two independent experiments). ** p<0.01, *** p<0.001. Error bars, means ± SEM. Scale bar, 20μm.

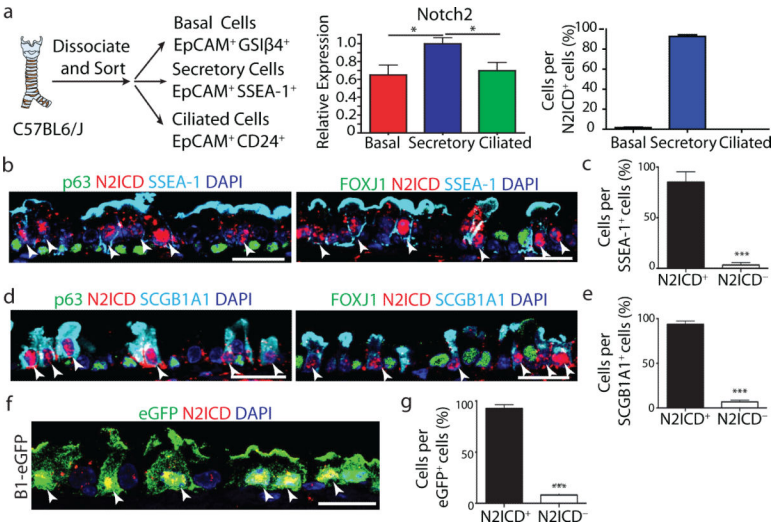

Figure 2. Secretory progenitor cells show tonic Notch2 activity at steady-state

a, Schematic representation of airway epithelial cell isolation. Relative mRNA expression of *Notch2* in sorted cells (n=3 mice) (middle). Percentage of each cell type per total N2ICD$^+$ cells (right). **b-e,** Immunostaining for p63 (left) or FOXJ1 (right) (green), SSEA-1 (b) or SCGB1A1 (d) (cyan) and N2ICD (red). Percentage of N2ICD$^+$ cells per total SSEA-1$^+$ (c) or SCGB1A1$^+$ (e) cells (n=3 mice). **f,** Immunostaining for eGFP (green) and N2ICD (red) in B1-eGFP mice. **g,** Percentage of N2ICD$^+$ cells per total eGFP$^+$ cells (n=3 mice). Nuclei, DAPI (blue). White arrowheads, double-positive cells. Images are representative of n=3 mice (biological replicates). * p<0.05, *** p<0.001. Error bars, means ± SEM. Scale bar, 20μm.

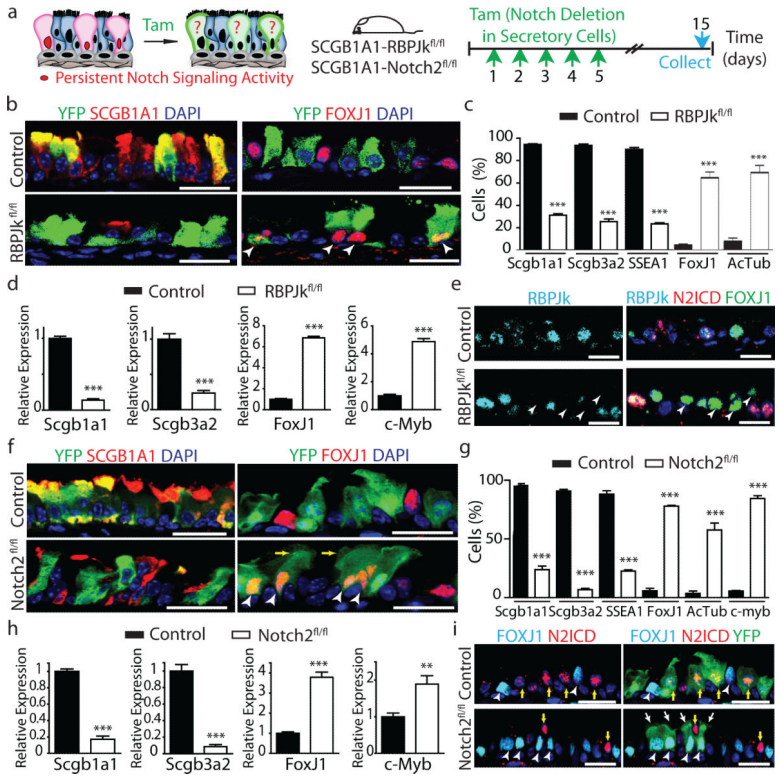

Figure 3. Tonic Notch2 activity is required to maintain secretory cells by preventing their differentiation into ciliated cells

a, Schematic representation of canonical Notch signaling inhibition in secretory cells. **b, f,** Immunostaining for YFP (green) and SCGB1A1 (left) or FOXJ1 (right) (red) in control (top) and experimental (bottom) mice (n=6 mice (b); n=7 mice (f)). White arrowheads, lineage labeled ciliated cells. **c, g,** Percentage of SCGB1A1$^+$, SCGB3A2$^+$, SSEA-1$^+$, FOXJ1$^+$, ACTUB$^+$ and C-MYB$^+$ cells per total YFP$^+$ cells. n=3 mice (c); n=7 mice (g). **d, h,** Relative mRNA expression of *Scgb1a1*, *Scgb3a2*, *FoxJ1* and *c-Myb* in control and experimental YFP$^+$ cells (n=3 mice). **e,** Immunostaining for RBPJk (cyan), N2ICD (red) and FOXJ1 (green). White arrowheads, RBPJk$^-$ N2ICD$^-$ FOXJ1$^+$ cells. **i,** Immunostaining for YFP (green), FOXJ1 (cyan) and N2ICD (red). White arrowheads, FOXJ1$^+$ cells. Yellow arrows, N2ICD$^+$ cells. White arrows, actual cilia in lineage labeled cells. Nuclei, DAPI (blue). n=biological replicates/condition repeated three times (three independent experiments). *** p<0.001; Error bars, means ± SEM. Scale bar, 20μm.

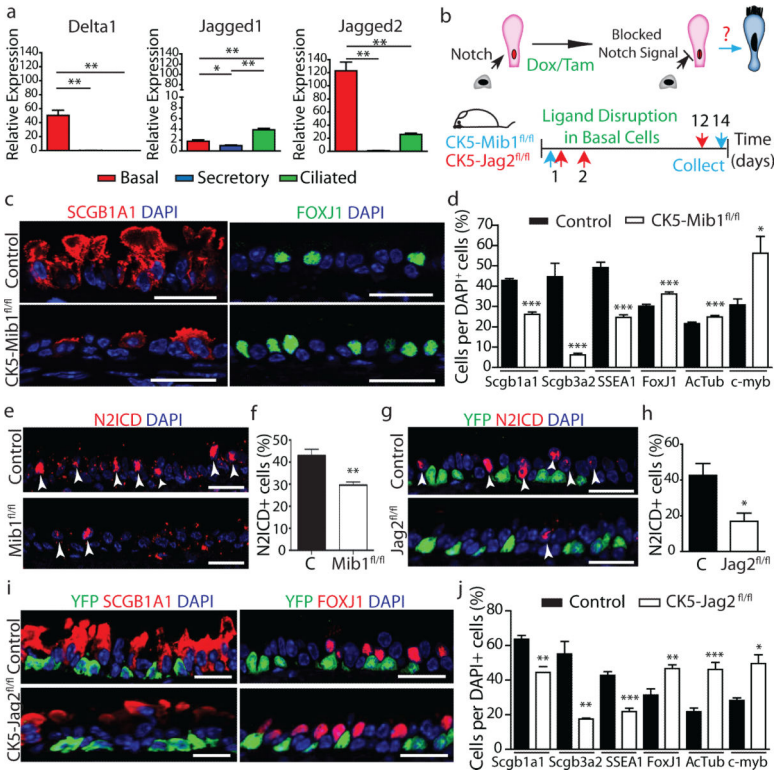

Figure 4. Basal cell Jagged2 expression is required to maintain secretory progenitors and prevent their differentiation into ciliated cells

a, Relative mRNA expression of *Delta1*, *Jagged1* and *Jagged2* in sorted cells (n=3 mice). **b,** Schematic representation of Notch ligand disruption in basal cells. **c,** Immunostaining for SCGB1A1 (red, left) and FOXJ1 (green, right) in control (top) and experimental CK5-Mib1$^{fl/fl}$ mice (bottom) (n=4 mice). **d,j** Percentage of SCGB1A1^{+}, SCGB3A2^{+}, SSEA-1^{+}, FOXJ1^{+}, ACTUB^{+} and C-MYB^{+} cells in control and experimental mice. n=4 mice (d); n=5 mice (j). **e,g** Immunostaining for N2ICD (red) and YFP (green, in **g**) n=4 mice (e); n=5 mice (g). White arrowheads, N2ICD^{+} cells. **f,h,** Percentage of N2ICD^{+} cells per total DAPI^{+} cells (n=4 mice; n=5 mice). **i,** Immunostaining for YFP (green) and SCGB1A1 (left) or FOXJ1 (right) (red) in control (top) and experimental CK5-Jag2$^{fl/fl}$ mice (bottom) (n=5). Nuclei, DAPI (blue). n=biological replicates/condition repeated twice (CK5-Mib1 mice) or three times (CK5-Jag2 mice). * p<0.05, ** p<0.01, *** p<0.001. Error bars, means ± SEM. Scale bar, 20μm.